

Adsorption isotherm modeling of carbendazim and flumetsulam onto homoionic-montmorillonite clays: comparison of linear and nonlinear models

Yassine EL MAATAOUI¹, Mohamadine EL M'RABET², Abdelkrim MAAROUFI^{1,*},
Hassan OUDDA³, Abdelmalek DAHCHOUR²

¹Laboratory of Composite Materials, Polymers, and Environment, Faculty of Sciences, University of Mohammed V, Rabat, Morocco

²Department of Fundamental and Applied Sciences, Hassan II Agronomy and Veterinary Institute, Rabat, Morocco

³Department of Chemistry, Faculty of Sciences, University of Ibn Tofail, Kenitra, Morocco

Received: 20.12.2016

Accepted/Published Online: 13.03.2017

Final Version: 05.09.2017

Abstract: This study deals with the adsorption of two pesticides, carbendazim and flumetsulam, from aqueous solutions onto four homoionic-montmorillonite clays (Ag^+ , Zn^{2+} , Cu^{2+} , and H^+). Equilibrium adsorption isotherm data were analyzed using Freundlich, Dubinin–Radushkevich, and Temkin isotherms. Linear and nonlinear fitting methods were compared to determine the best-fitting isotherms for the experimental data. Three error analysis methods were used to evaluate the data for each method: the coefficient of determination (R^2), sum of squared errors (SSE), and chi-square test (χ^2). Equilibrium adsorption isotherms exhibited that the carbendazim adsorption mainly involved cation exchange with homoionic-montmorillonite adsorbents. However, for flumetsulam, the main mechanisms were possibly the cation bridging by Ag^+ , Zn^{2+} , and Cu^{2+} cations and the surface complexation reactions of the adsorption on homoionic-montmorillonite (H^+) adsorbent. The modeling results showed that the nonlinear Freundlich model could fit the data better than the Dubinin–Radushkevich or Temkin models, with relatively higher R^2 and smaller SSE and χ^2 values. Thus, the nonlinear method is a better way to obtain the isotherm parameters.

Key words: Adsorption, homoionic-montmorillonite, carbendazim, flumetsulam, modeling analysis

1. Introduction

Pesticides are considered as one of the main potential environmental hazards, as they are toxic to human beings, animals, and plants¹ Moreover, pesticides are carcinogenic in nature and they are sometimes nonbiodegradable^{2–5} The increased population density is projected to increase the demand for food production. Thus, we need to grow food on even less land, with less water and with increasing use of pesticides for controlling pests⁶ Therefore, high levels of these chemicals may be causing contamination in both irrigation and drainage water. These compounds have been recently detected in sewage effluents, surface water, ground water, and sometimes even in drinking water^{7–10}

Carbendazim is a fungicide from the benzimidazole group used to control a broad range of diseases on arable crops. Carbendazim is a weak base, with $\text{Log}K_{ow}$ of 1.48 at pH 7 (20 °C), and a basic $\text{p}K_a$ of 4.2^{11,12} It has been found to induce endocrine-disrupting effects^{11,13} Flumetsulam is a member of the sulfonanilide family of herbicides that is used for postemergence control for undersown wheat and certain legume crops and

*Correspondence: maaroufi@fsr.ac.ma

pastures. It acts by inhibiting the enzyme acetolactate synthase, which is essential for amino acid synthesis in plants^{14,15} Flumetsulam is a weak acid, with $\text{Log}K_{ow}$ of 0.21 at pH 7 (20 °C) and $\text{p}K_a$ of 4.6,^{14,15} and it exists in both neutral and anionic forms in most agronomic soils, with a higher proportion of the anionic form in soils with higher pH¹⁶ In aqueous solutions, the two molecules can undergo protonation-deprotonation reactions and form cation or anion species, which depends strongly on medium pH. Figure 1 shows the distribution and molecular structure of different species for carbendazim and flumetsulam as calculated using MarvinSketch software (Version 16.1.4, ChemAxon, <http://www.chemaxon.com>). When the solution pH is below the $\text{p}K_{a1}$ constant ($\text{p}K_{a1} = 4.2$) of the equilibrium between form 1 and form 2, the carbendazim molecules mostly exist as cations (form 1). On the contrary, the major form of carbendazim molecules when the solution pH is higher than the $\text{p}K_{a2}$ constant ($\text{p}K_{a2} = 9.6$) of the equilibrium between form 2 and form 3 is the anionic form (form 3). Between the two $\text{p}K_a$ constants ($\text{p}K_{a1} < \text{pH} < \text{p}K_{a2}$), the neutral form (form 2) is dominant. However, flumetsulam molecules mainly exist in the neutral form (form 1) when the pH is below the $\text{p}K_a$ constant ($\text{p}K_a = 8.8$) of the equilibrium between forms 1 and 2. Otherwise, the anionic form (form 2) is dominant ($\text{pH} > 8.8$).

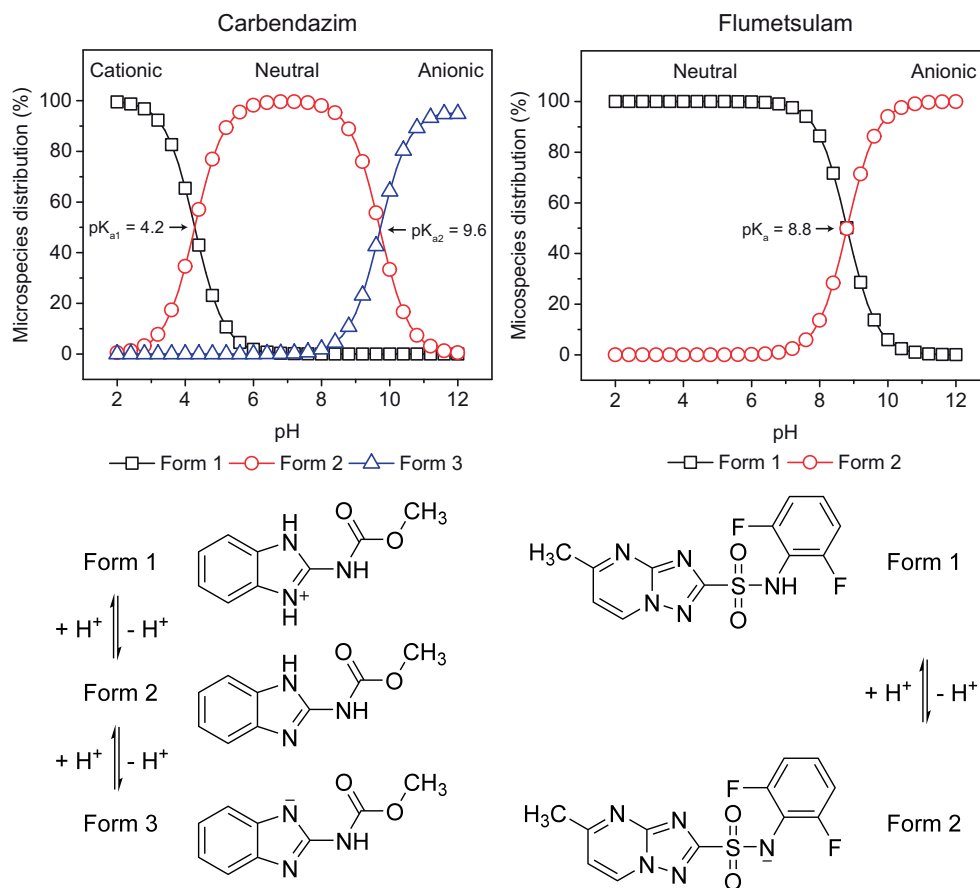


Figure 1. Structure and different species forms of carbendazim and flumetsulam at different pH levels.

The environmental fate of pesticides and their biological activities are largely affected by adsorption processes in soil^{17,18} Clay minerals have great potential to adsorb pollutants due to their layered structure, high cation exchange capacity, and large specific surface area. Soil clay minerals and organic matter have been shown to be the primary adsorbents for pesticides and other organic pollutants in soil as well as with the

presence of exchangeable cations^{19–21} Sorbent and sorbate equilibrium relationships are described by sorption isotherms, which indicate the capacity of a sorbent for a sorbate. Linear transformed isotherm equations have been widely used to confirm isotherm experimental data using coefficients of determination. Linear regression is frequently used to determine the best-fitting isotherm. Recently, several error analysis methods, such as the coefficient of determination (R^2), the chi-square test (χ^2), and the sum of squared errors (SSE), have been used to determine the best-fitting isotherm equation^{22,23}

In this research, the linear and nonlinear methods of three isotherm models, Freundlich, Dubinin–Radushkevich, and Temkin, were compared for the experimental data of carbendazim and flumetsulam adsorption on homoionic-montmorillonite clays. Three error analysis methods, R^2 , SSE, and χ^2 , were used to evaluate the data for each fitting method.

2. Results and discussion

Equilibrium adsorption isotherms of carbendazim and flumetsulam by homoionic-montmorillonite (M-H, M-Ag, M-Zn, and M-Cu) samples are shown in Figure 2. As can be seen, isotherms for both molecules are C types according to the Giles classification,²⁴ indicating a good affinity of the adsorbent for the adsorbate. The linearity shows that the number of sites for adsorption remains constant; as more solute is adsorbed, more sites are created²⁴

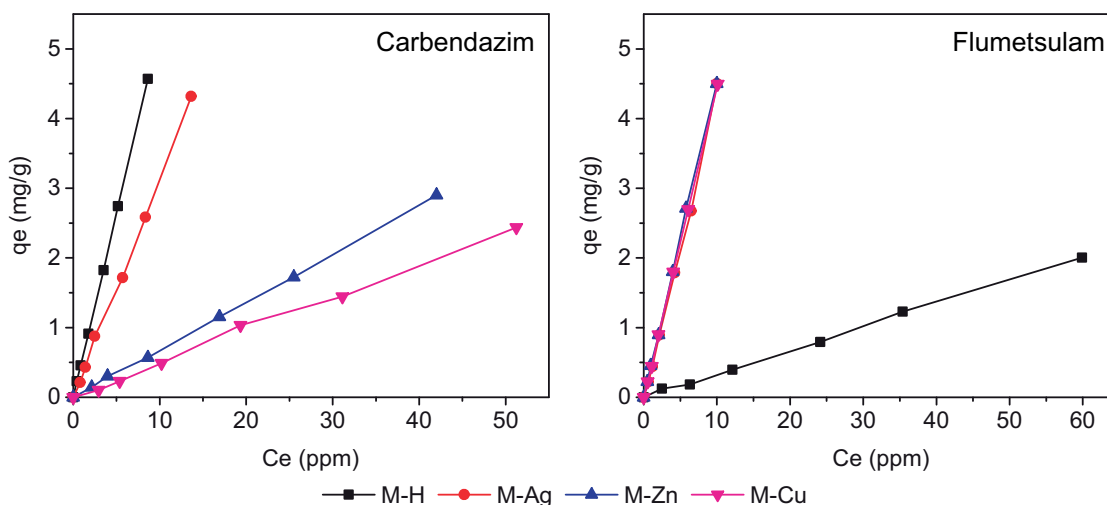


Figure 2. Linear adsorption isotherms (experimental data) of carbendazim and flumetsulam.

Figure 3 presents the distribution charge of carbendazim and flumetsulam molecules as a function of the pH values calculated using MarvinSketch software. The isoelectric point (IEP) is the pH at which the molecule has a net charge equal to zero. At pH values below the IEP constant, the molecule has a net positive charge. However, it has a net negative charge when the pH is above the IEP constant. The IEP values of carbendazim and flumetsulam are respectively equal to 7.0 and 2.7.

Concerning the carbendazim, the M-H and M-Ag samples show higher affinity to carbendazim molecules than M-Zn and M-Cu. Indeed, as given in Table 1, the order of the four adsorbents according to the distribution coefficient (K_d) values is M-H > M-Ag >> M-Zn > M-Cu. Thus, the effect of monovalent cations (H^+ and Ag^+) is different from the adsorption from divalent cations (Zn^{2+} and Cu^{2+}). However, the carbendazim molecule in aqueous solution is positively charged when $pH < IEP$ (7.0) (isoelectric point of carbendazim).

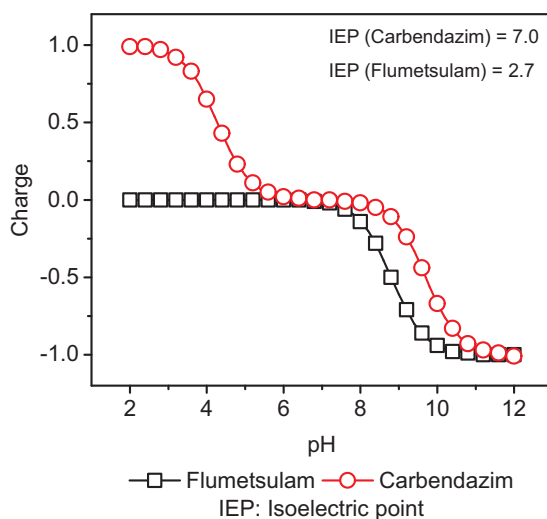


Figure 3. Isoelectric point of carbendazim and flumetsulam.

The adsorption of carbendazim on the negatively charged surface of montmorillonite mainly involves the cation exchange with the interlayer exchange cations present in clay minerals²⁵ The difference in adsorption capacity seems to indicate that the divalent cations present more difficulties than the monovalent cations to be exchanged by carbendazim in the cation exchange mechanism^{19,26} The exchangeability of interlayer cations follows the order $H^+ > Ag^+ \gg Zn^{2+} > Cu^{2+}$. However, for flumetsulam, the affinity of M-Ag, M-Zn, and M-Cu samples to flumetsulam molecules is higher than that for the M-H sample. The order of these adsorbents for the K_d values (Table 1) is M-Zn > M-Cu > M-Ag \gg M-H. The adsorbents exchanged by Zn^{2+} , Cu^{2+} , and Ag^+ have similar adsorption capacities. In addition to the cation exchange and surface complexation reactions, the Zn^{2+} , Cu^{2+} , and Ag^+ cations are probably acting as bridge ions between flumetsulam species and montmorillonite sites^{27–30} In aqueous solution, the flumetsulam molecule exists in neutral and negative forms. It becomes more and more negatively charged when $pH > IEP$ (2.7) (isoelectric point of flumetsulam). The presence of montmorillonite clays with the flumetsulam molecule may prevent adsorption because of the charge repulsion between the negatively charged montmorillonite surface and the flumetsulam molecule^{31,32} Moreover, it can interact with the positive sites at the edge of the montmorillonite clays through surface complexation reactions^{33,34} This might be the main mechanism involved in the adsorption of flumetsulam on M-H.

Table 1. Distribution coefficient of carbendazim and flumetsulam with homoionic clays.

K_d *	M-H	M-Ag	M-Zn	M-Cu
Carbendazim	0.530 ± 0.013	0.308 ± 0.028	0.069 ± 0.004	0.046 ± 0.006
Flumetsulam	0.035 ± 0.007	0.405 ± 0.035	0.455 ± 0.017	0.434 ± 0.020

* K_d average value \pm standard deviation (n = 6).

2.1. Linear fitting of isotherm models

Table 2 shows the Freundlich, Dubinin–Radushkevich, and Temkin values of the corresponding isotherm parameters determined by linear isotherm fitting for each adsorbent with their R^2 , SSE, and χ^2 values. As can be seen, for carbendazim and flumetsulam, R^2 values for the Freundlich isotherm model are higher as

compared to the Temkin and Dubinin–Radushkevich isotherm models. However, the R^2 values of the Dubinin–Radushkevich isotherm model are the lowest. On the other hand, the SSE and χ^2 values are the lowest for the Freundlich isotherm as compared to the other models. This means that the Freundlich isotherm model can generate a satisfactory fit to the experimental data, while the Temkin and Dubinin–Radushkevich models cannot. Comparison by the best linear analysis fits of the isotherm gives the following order: Freundlich > Temkin > Dubinin–Radushkevich.

Table 2. Linear isotherm fitting with Freundlich, Dubinin–Radushkevich, and Temkin models.

Carbendazim					
		M-H	M-Ag	M-Cu	M-Zn
Freundlich	n	1.0129	0.9656	0.9130	1.0096
	n_F	0.9873	1.0356	1.0953	0.9905
	K_F (mg/g)	0.5355	0.2934	0.0354	0.0705
	R^2	0.9997	0.9946	0.9936	0.9981
	SSE	0.0020	0.0349	0.0452	0.0124
	χ^2	5.0945×10^{-4}	0.0087	0.0113	0.0031
Dubinin–Radushkevich	K_{ad} (mol ² /J ²)	3.9450×10^{-8}	1.1218×10^{-7}	6.2916×10^{-7}	3.9482×10^{-7}
	q_s (mg/g)	2.8996	5.2105	79.8006	19.9705
	E (KJ/mol)	3.5601	2.1112	0.8915	1.1253
	R^2	0.7525	0.8552	0.8948	0.8513
	SSE	1.5777	0.9362	0.7441	0.9443
	χ^2	0.3944	0.2341	0.1860	0.2361
Temkin	B_T	1.3276	1.3317	0.7703	0.8488
	A_T (L/g)	1.7914	1.0173	0.2651	0.3623
	b_T (KJ/mol)	1.8724	1.8666	3.2273	2.9288
	R^2	0.8466	0.8757	0.8888	0.8520
	SSE	2.0879	1.5088	0.4349	0.8084
	χ^2	0.5220	0.3772	0.1087	0.2021
Flumetsulam					
		M-H	M-Ag	M-Cu	M-Zn
Freundlich	n	1.0891	0.9311	0.9683	0.9979
	n_F	0.9182	1.0740	1.0327	1.0021
	K_F (mg/g)	0.0435	0.3748	0.4204	0.4543
	R^2	0.9788	0.9989	0.9994	0.9989
	SSE	0.1254	0.0074	0.0040	0.0071
	χ^2	0.0313	0.0019	9.9769×10^{-4}	0.0018
Dubinin–Radushkevich	K_{ad} (mol ² /J ²)	4.1915×10^{-7}	7.5265×10^{-8}	6.1951×10^{-8}	5.6198×10^{-8}
	q_s (mg/g)	13.5801	3.9690	3.5253	3.4243
	E (KJ/mol)	1.0922	2.5775	2.8409	2.9828
	R^2	0.6995	0.8015	0.7855	0.8009
	SSE	1.7810	1.2882	1.3800	1.2727
	χ^2	0.4453	0.3221	0.3450	0.3182
Temkin	B_T	0.5614	1.4197	1.3765	1.3372
	A_T (L/g)	0.2788	1.2519	1.3933	1.5165
	b_T (KJ/mol)	4.4279	1.7510	1.8060	1.8590
	R^2	0.8224	0.8576	0.8660	0.8599
	SSE	0.4683	1.8812	1.7674	1.8525
	χ^2	0.1171	0.4703	0.4419	0.4631

According to the Freundlich isotherm model, the comparison of the data of the four homoionic clays reveals that the order of the best fits from higher R^2 and lower SSE and χ^2 to lower R^2 and higher SSE and χ^2 is M-H > M-Zn > M-Ag > M-Cu for carbendazim and M-Cu > M-Zn > M-Ag > M-H for flumetsulam.

2.2. Nonlinear fitting of isotherm models

Table 3 shows different isotherm parameter values of the Freundlich, Dubinin–Radushkevich, and Temkin models for each adsorbent with their R^2 , SSE, and χ^2 values obtained with nonlinear isotherm fitting. As in the case of linear isotherm fitting analysis, in nonlinear isotherm fitting treatment, the Freundlich isotherm model has the highest R^2 and the lowest SSE and χ^2 values as compared to other isotherm models.

In general, the R^2 values of the Dubinin–Radushkevich isotherm model are lower than those of the Freundlich or Temkin isotherm models. The order of the best fits of the data of the four homoionic clays from higher R^2 and lower SSE and χ^2 to lower R^2 and higher SSE and χ^2 according to the Freundlich isotherm model is M-H > M-Zn > M-Ag > M-Cu for carbendazim and M-Cu > M-Zn > M-Ag > M-H for flumetsulam.

2.3. Comparison between linear and nonlinear fitting

According to the Freundlich isotherm model for both molecules (Table 2 and 3), the R^2 values for nonlinear fitting analysis are higher than the corresponding R^2 values obtained by linear fitting analysis. Moreover, the corresponding SSE and χ^2 values are lower.

Concerning the Dubinin–Radushkevich isotherm model (Table 2 and 3), for carbendazim molecules, the R^2 values for the linear fitting isotherm are higher than those obtained by nonlinear fitting analysis, except that the value for M-H is lower. Meanwhile, the SSE and χ^2 values for M-H and M-Ag are higher for nonlinear fitting analysis than for linear fitting analysis. However, for flumetsulam molecules, the R^2 values are higher than the corresponding R^2 values obtained by linear fitting analysis for all adsorbents, whereas the SSE and χ^2 values are higher for M-Ag, M-Cu, and M-Zn for nonlinear fitting analysis than the values for linear fitting analysis and lower for M-H. On the other hand, the R^2 , SSE, and χ^2 values for nonlinear fitting analysis are equal to the values obtained by linear fitting analysis for the Temkin isotherm model in all cases. These results indicate that the Freundlich isotherm model is the best to fit the experimental data using nonlinear analysis while the Dubinin–Radushkevich and Temkin isotherm models are the worst for both fitting methods. Linear and nonlinear fitting of experimental data into the Dubinin–Radushkevich and Temkin isotherm models may cause great fluctuation of R^2 , and the predicted parameters may induce deviation.

In conclusion, equilibrium adsorption isotherms of carbendazim molecules showed that the adsorption capacities of the adsorbents exchanged with monovalent cations (H^+ and Ag^+) are higher than those with bivalent cations (Zn^{2+} and Cu^{2+}). The adsorption of carbendazim mainly involves cation exchange with homoionic-montmorillonite adsorbents. However, for flumetsulam, the adsorption capacities of homoionic-montmorillonite adsorbents (M-Ag, M-Zn, and M-Cu) are higher than that of the M-H adsorbent. The Ag^+ , Zn^{2+} , and Cu^{2+} cations are probably acting as bridge ions between flumetsulam species and montmorillonite sites. The surface complexation reactions are possibly the main mechanism involved in the adsorption of flumetsulam on M-H adsorbent. The results of regression analyses showed that the Freundlich model could fit the data better than the Dubinin–Radushkevich or the Temkin model. Moreover, the Freundlich model fit the experimental data best by nonlinear analysis. Therefore, the nonlinear isotherm model is more powerful and viable in modeling the adsorption isotherm data.

Table 3. Nonlinear isotherm fitting with Freundlich, Dubinin–Radushkevich and Temkin models.

Carbendazim					
		M-H	M-Ag	M-Cu	M-Zn
Freundlich	n	0.9894	0.9856	1.0206	0.9875
	n_F	1.0107	1.0146	0.9798	1.0127
	K_F (mg/g)	0.5180	0.3028	0.0515	0.0657
	R^2	0.9999	0.9980	0.9962	0.9996
	SSE	0.0012	0.0190	0.0150	0.0021
	χ^2	2.9014×10^{-4}	0.0048	0.0037	5.2012×10^{-4}
Dubinin–Radushkevich	K_{ad} (mol ² /J ²)	0.0205	0.0082	5.7616×10^{-4}	8.6668×10^{-4}
	q_s (mg/g)	1.0315	0.9645	0.5545	0.6492
	E (KJ/mol)	0.0049	0.0078	0.0295	0.0240
	R^2	0.8370	0.8445	0.8267	0.8436
	SSE	2.2188	1.8878	0.6775	0.8542
	χ^2	0.5547	0.4720	0.1694	0.2136
Temkin	B_T	1.3276	1.3318	0.7703	0.8488
	A_T (L/g)	1.7914	1.0173	0.2651	0.3623
	b_T (KJ/mol)	1.8725	1.8666	3.2272	2.9287
	R^2	0.8466	0.8757	0.8888	0.8520
	SSE	2.0879	1.5088	0.4349	0.8084
	χ^2	0.5220	0.3772	0.1087	0.2021
Flumetsulam					
		M-H	M-Ag	M-Cu	M-Zn
Freundlich	n	0.9992	0.9216	0.9956	1.0142
	n_F	1.0008	1.0851	1.0044	0.9860
	K_F (mg/g)	0.0336	0.3658	0.4406	0.4675
	R^2	0.9983	0.9984	0.9998	0.9992
	SSE	0.0046	0.0206	0.0022	0.0107
	χ^2	0.0011	0.0052	5.3729×10^{-4}	0.0027
Dubinin–Radushkevich	K_{ad} (mol ² /J ²)	4.1970×10^{-4}	0.0157	0.0149	0.0150
	q_s (mg/g)	0.4600	0.9652	1.0173	1.0356
	E (KJ/mol)	0.0345	0.0056	0.0058	0.0058
	R^2	0.8279	0.8631	0.8348	0.8238
	SSE	0.4537	1.8082	2.1781	2.3304
	χ^2	0.1134	0.4521	0.5445	0.5826
Temkin	B_T	0.5614	1.4197	1.3765	1.3372
	A_T (L/g)	0.2788	1.2519	1.3933	1.5165
	b_T (KJ/mol)	4.4280	1.7510	1.8060	1.8590
	R^2	0.8224	0.8576	0.8660	0.8599
	SSE	0.4683	1.8812	1.7674	1.8525
	χ^2	0.1171	0.4703	0.4419	0.4631

3. Experimental

3.1. Clay preparation

Montmorillonite clay (K10 with a fraction of $<2 \mu\text{m}$) was obtained from Fluka Chemie AG (Switzerland). Homoionic-montmorillonite clays were prepared using a published procedure³⁵ A suitable amount of the montmorillonite clay was dispersed in solutions of Ag^+ , Zn^{2+} , Cu^{2+} , and H^+ ions as chlorides. The samples were

then washed several times with distilled water to remove excess electrolytes. Homoionic clays were dried at 60 °C and powdered in a mortar to obtain finer grains before the experiments.

3.2. Reagents and solutions

Certified standards of carbendazim and flumetsulam, purity greater than 97%, were supplied by Sigma-Aldrich. Stock standard solutions were prepared in methanol at 1000 mg/L concentration. Working solutions of these compounds were prepared by further diluting the stock solutions in deionized water. Calibration standards were prepared at 5.0, 10.0, 20.0, 40.0, 60.0, and 100.0 mg/L concentrations by dilution with deionized water. Methanol, silver chloride, zinc chloride, copper(II) chloride, and hydrochloric acid were purchased from Sigma-Aldrich. All the reagents were of analytical grade.

3.3. Adsorption experiment

Equilibrium isotherms were determined by shaking a fixed mass (0.2 g) of homoionic clays (M-Ag, M-Zn, M-Cu, and M-H) with 10 mL of carbendazim and flumetsulam solutions in a proper range of concentrations (5 to 100 mg/L) at 25 °C and without pH adjustment. As a function of solution concentrations, the initial pH (natural pH) of different solutions varied from 6 to 7.5 (± 0.1). These samples were placed in appropriate tubes. A series of such tubes was then shaken for 24 h. The homoionic clays were separated by centrifugation for 30 min at 2000 rpm and filtered with 0.45- μ m membrane filters. Solutions were then analyzed for the remaining adsorbate concentration using a spectrophotometer at λ_{max} of 286 nm and 260 nm for carbendazim and flumetsulam, respectively.

The capacity of adsorption (q_e) was calculated using the following equation:

$$q_e = (C_0 - C_e) V / M, \quad (1)$$

where the q_e parameter is the capacity of adsorption at equilibrium (mg/g) and C_0 and C_e are the initial and equilibrium concentrations of adsorbate in solution (mg/L), respectively. V (L) is the solution volume and M (g) is the homoionic-montmorillonite clay weight.

3.4. Equilibrium isotherm

A variety of models can be used to describe adsorption processes. Empirical adsorption isotherm equations are excellent for describing experimental sorption data. The equation parameters of these equilibrium models provide the sorption mechanisms, surface properties, and affinities of the sorbent. In the present study, three isotherm models were tested using carbendazim and flumetsulam as adsorbate molecules.

3.4.1. Freundlich isotherm

The Freundlich isotherm has been largely used to describe solid-liquid sorption systems. It is based on multilayer adsorption on heterogeneous surfaces^{36,37} The nonlinear Freundlich isotherm is commonly presented as:³⁸

$$q_e = K_F C_e^{1/n}. \quad (2)$$

The linearized form of Eq. (2) is:

$$\ln(q_e) = 1/n \ln(C_e) + \ln(K_F), \quad (3)$$

where q_e is the adsorbed amount of adsorbate per gram of sorbent (mg/g) and C_e is the equilibrium concentration of the adsorbate in the solution (mg/L). K_F and n are the Freundlich constants that represent the adsorption capacity and adsorption strength, respectively. The magnitude of $n_F = 1/n$ quantifies the favorability of adsorption and the degree of heterogeneity of the surface³⁹ In the linear form, it will have a straight line with a slope of $1/n$ and an intercept of $\ln(K_F)$.

The nonlinear equation reduces to a linear adsorption isotherm when parameter $1/n = 1$ ³⁶ The linear adsorption isotherm equation becomes:

$$q_e = K_d C_e, \quad (4)$$

where q_e and C_e , as indicated previously, are the capacity of adsorption and the equilibrium concentration, respectively. K_d is the distribution coefficient, which is defined as the ratio of the amount adsorbed and remaining of the adsorbate in solution at equilibrium.

3.4.2. Dubinin–Radushkevich isotherm

The Dubinin–Radushkevich isotherm is usually applied to adsorption data to determine the predominant adsorption type (physical or chemical) with the mean free energy E (KJ/mol), which describes the energy necessary for removing a molecule from its location in the sorption space to infinity:^{40,41}

$$E = 1/\sqrt{2k_{ad}}. \quad (5)$$

when $E < 8$ kJ/mol, the predominant mechanism is physical interaction, and it is a chemical ion-exchange interaction if $8 \text{ kJ/mol} \leq E \leq 16 \text{ kJ/mol}$.

The nonlinear form of this model is:

$$q_e = (q_s) \exp(-k_{ad}\varepsilon^2). \quad (6)$$

The linear form of Eq. (6) can be described as follows:

$$\ln(q_e) = \ln(q_s) - k_{ad}\varepsilon^2, \quad (7)$$

where q_e is the amount adsorbed at equilibrium (mg/g), q_s is theoretical isotherm saturation capacity (mg/g), and k_{ad} is the Dubinin–Radushkevich isotherm constant (mol^2/kJ). Values of q_s and k_{ad} are calculated from the slope and intercept of the plot $\ln q_e$ versus ε^2 . ε , the Polanyi potential, is calculated by Eq. (8):⁴²

$$\varepsilon = RT \ln [1 + 1/C_e]. \quad (8)$$

R , T , and C_e represent the gas constant (8.314 J/mol K), absolute temperature (K), and adsorbate equilibrium concentration (mg/L), respectively.

3.4.3. Temkin isotherm

The Temkin isotherm has generally been applied in the following form:^{40,43}

$$q_e = (RT/b_T) \ln A_T C_e. \quad (9)$$

The linearized form is:

$$q_e = (RT/b_T) \ln A_T + (RT/b_T) \ln C_e, \quad (10)$$

with:

$$B_T = (RT/b_T), \quad (11)$$

where R, T, and b_T represent the gas constant (8.314 J/mol K), absolute temperature (K), and Temkin isotherm constant (KJ/mol), respectively. A_T is the Temkin isotherm equilibrium binding constant (L/g) and C_e is the equilibrium concentration (mg/L).

3.5. Error analysis

To evaluate the fit model of adsorption isotherms, the data are analyzed using error analysis functions. The R^2 , SSE, and χ^2 values were determined for linear and nonlinear isotherms:^{22,37,44}

$$R^2 = \sum (q_c - \bar{q}_e)^2 / \left(\sum (q_c - \bar{q}_e)^2 + \sum (q_c - q_e)^2 \right), \quad (12)$$

$$SSE = \sum (q_c - q_e)^2, \quad (13)$$

$$\chi^2 = \sum (q_e - q_c)^2 / q_c, \quad (14)$$

where q_c is the equilibrium capacity obtained from the model (mg/g) and q_e is experimental data of the equilibrium capacity (mg/g).

References

1. Amaraneni, S. R. *Environ. Int.* **2006**, *32*, 294-302.
2. Gupta, V. K.; Ali, I.; Suhas; Saini, V. K. *J. Colloid Interf. Sci.* **2006**, *299*, 556-563.
3. Mostafalou, S.; Abdollahi, M. *Toxicol. Appl. Pharm.* **2013**, *268*, 157-177.
4. Wu, C.; Luo, Y.; Gui, T.; Huang, Y. *Sci. Total Environ.* **2014**, *470-471*, 1047-1055.
5. Papadakis, E. N.; Vryzas, Z.; Kotopoulou, A.; Kintzikoglou, K.; Makris, K. C.; Papadopoulou-Mourkidou, E. *Ecotox. Environ. Safe.* **2015**, *116*, 1-9.
6. Popp, J.; Peto, K.; Nagy, J. *Agron. Sustain. Dev.* **2013**, *33*, 243-255.
7. Net, S.; Dumoulin, D.; El-Osmani, R.; Rabodonirina, S.; Ouddane, B. *Int. J. Environ. Res.* **2014**, *8*, 1159-1170.
8. Lari, S. Z.; Khan, N. A.; Gandhi, K. N.; Meshram, T. S.; Thacker, N. P. *J. Environ. Health Sci. Eng.* **2014**, *12*, 1-7.
9. Silva, E.; Daam, M. A.; Cerejeira, M. J. *Chemosphere* **2015**, *135*, 394-402.
10. Nam, S. W.; Jo, B. I.; Yoon, Y.; Zoh, K. D. *Chemosphere* **2014**, *95*, 156-165.
11. Bányiová, K.; Nečasová, A.; Kohoutek, J.; Justan, I.; Čupr, P. *Chemosphere* **2016**, *145*, 148-156.
12. Liu, K.; Pan, X.; Han, Y.; Tang, F.; Yu, Y. *Sci. Total Environ.* **2012**, *438*, 26-32.
13. Rama, E. M.; Bortolan, S.; Vieira, M. L.; Gerardin, D. C. C.; Moreira, E. G. *Regul. Toxicol. Pharm.* **2014**, *69*, 476-486.
14. Felix, J.; Doohan, D. J.; Ditmarsen, S. C.; Schultz, M. E.; Wright, T. R.; Flood, B. R.; Rabaey, T. L. *Crop Prot.* **2005**, *24*, 790-797.
15. Strebe, T. A.; Talbert, R. E. *Weed Sci.* **2001**, *49*, 806-813.
16. Fontaine, D. D.; Lehmann, R. G.; Miller, J. R. *J. Environ. Qual.* **1991**, *20*, 759-762.

17. Larsbo, M.; Löfstrand, E.; De Veer, D. V. A.; Ulén, B. *J. Contam. Hydrol.* **2013**, *147*, 73-81.
18. Kodešová, R.; Kočárek, M.; Kodeš, V.; Drábek, O.; Kozák, J.; Hejtmánková, K. *J. Hazard. Mater.* **2011**, *186*, 540-550.
19. Yan, W.; Hu, S.; Jing, C. *J. Colloid Interf. Sci.* **2012**, *372*, 141-147.
20. Gámiz, B.; López-Cabeza, R.; Facenda, G.; Velarde, P.; Hermosín, M. C.; Cox, L.; Celis, R. *Agric. Ecosyst. Environ.* **2016**, *230*, 32-41.
21. Ayari, F.; Srasra, E.; Trabelsi-Ayadi, M. *Desalination* **2007**, *206*, 499-506.
22. Ho, Y. S. *Pol. J. Environ. Stud.* **2006**, *15*, 81-86.
23. Karadag, D.; Koc, Y.; Turan, M.; Ozturk, M. *J. Hazard. Mater.* **2007**, *144*, 432-437.
24. Giles, C. H.; MacEwan, T. H.; Nakhwa, S. N.; Smith, D. *J. Chem. Soc.* **1960**, 3973-3993.
25. Cancela, G. D.; Taboada, E. R.; Sanchezrasero, F. *J. Soil Sci.* **1992**, *43*, 99-111.
26. Ma, Y. L.; Xu, Z. R.; Guo, T.; You, P. *J. Colloid Interf. Sci.* **2004**, *280*, 283-288.
27. Li, Z.; Hong, H.; Liao, L.; Ackley, C. J.; Schulz, L. A.; MacDonald, R. A.; Mihelich, A. L.; Emard, S. M. *Colloid. Surface. B* **2011**, *88*, 339-344.
28. Zhao, Y.; Geng, J.; Wang, X. *Ecotoxicology* **2011**, *20*, 1141-1147.
29. Peruchi, L. M.; Fostier, A. H.; Rath, S. *Chemosphere* **2015**, *119*, 310-317.
30. Parolo, M. E.; Avena, M. J.; Pettinari, G. R.; Baschini, M. T. *J. Colloid Interf. Sci.* **2012**, *368*, 420-426.
31. Wang, C. J.; Li, Z.; Jiang, W. T.; Jean, J. S.; Liu, C. C. *J. Hazard. Mater.* **2010**, *183*, 309-314.
32. Wu, Q.; Li, Z.; Hong, H. *Appl. Clay Sci.* **2013**, *74*, 66-73.
33. Figueroa, R. A.; Mackay, A. A. *Environ. Sci. Technol.* **2005**, *39*, 6664-6671.
34. Ramos, M. E.; Huertas, F. J. *Appl. Clay Sci.* **2013**, *80-81*, 10-17.
35. González García, F.; González García, S. **1953**, 925-992.
36. Goldberg, S. In *Chemical Processes in Soils*; Tabatabai, M. A.; Sparks, D. L., Eds. Soil Science Society of America: Madison, WI, USA, 2005, pp. 489-517.
37. Ho, Y. S.; Chiu, W. T.; Wang, C. C. *Bioresource Technol.* **2005**, *96*, 1285-1291.
38. Freundlich, H. M. F. *Z. Phys. Chem.* **1906**, *57*, 385-470.
39. Xu, J.; Wang, L.; Zhu, Y. *Langmuir* **2012**, *28*, 8418-8425.
40. Foo, K. Y.; Hameed, B. H. *Chem. Eng. J.* **2010**, *156*, 2-10.
41. Sdiri, A.; Higashi, T.; Hatta, T.; Jamoussi, F.; Tase, N. *Chem. Eng. J.* **2011**, *172*, 37-46.
42. Akçay, G.; Kılınç, E.; Akçay, M. *Colloid. Surface. A* **2009**, *335*, 189-193.
43. Ho, Y. S.; Porter, J. F.; McKay, G. *Water Air Soil Poll.* **2002**, *141*, 1-33.
44. Han, R.; Zhang, J.; Han, P.; Wang, Y.; Zhao, Z.; Tang, M. *Chem. Eng. J.* **2009**, *145*, 496-504.